Insulator-metal transition and anomalous sign reversal of the dominant charge carriers in perovskite $BaTiO_{3-\delta}$

T. Kolodiazhnyi*
Opto-Electronic Group, National Institute for Materials Science, 1-1 Namiki, Tsukuba, Ibaraki 305-0044, Japan
(Received 9 April 2008; revised manuscript received 20 May 2008; published 14 July 2008)

Dc resistivity, magnetic susceptibility, and Hall and Seebeck coefficients were measured in the 2–400 K range on perovskite $BaTiO_{3-\delta}$ single crystals with electron concentration of $9.8\times10^{17}-3.5\times10^{20}$ cm^{-3}. The insulator-metal transition in $BaTiO_{3-\delta}$ was found at critical electron concentration $n_c\approx1.6\times10^{20}$ cm^{-3}. In contrast to $SrTiO_{3-\delta}$, both Hall and Seebeck coefficients of metallic $BaTiO_{3-\delta}$ show strong temperature dependence below 290 K which culminates by a sign reversal from negative to positive. The temperature of the sign reversal anomaly is concentration dependent and increases with n. Magnetic susceptibility of metallic samples shows anomalous decrease upon cooling below 300 K. It is proposed that the low-temperature p-type conductivity in $BaTiO_{3-\delta}$ may be attributed to the charge-carrier contributions from the two electronic bands separated by a narrow (3–7 meV) energy gap.

DOI: 10.1103/PhysRevB.78.045107 PACS number(s): 71.20.−b, 71.30.+h, 71.70.−d, 72.20.Pa

I. INTRODUCTION

Since their discovery more than 60 years ago, $BaTiO_3$ and $SrTiO_3$ are among the most extensively studied and widely utilized perovskites. Yet, a number of fundamental questions regarding their crystal structure as well as dielectric and electronic properties continue to challenge research community.[1]

Theoretical calculations[2,3] predict similar structure of the lowest conduction and highest valence bands in $SrTiO_3$ and $BaTiO_3$. These bands are formed predominantly by the Ti $3d$ and O $2p$ orbitals. Kahn and Leyendecker[2] using the linear combination of atomic orbitals (LCAO) method found six lowest conduction-band ellipsoids in the cubic Sr(Ba) TiO_3 lying along the ⟨100⟩ directions of the **k** space and centered at the X points of the Brillouin zone. In contrast, the APW calculations performed by Mattheiss[3] suggest a single valley model with a minimum at the Γ point. The most recent *ab initio* calculations on $SrTiO_3$ confirmed that the conduction-band minimum is located at the Γ point but owing to the weak dispersion, the energy difference between the $\Gamma_{25'}$ and X_3 points is relatively small, i.e., 0.134 eV.[4] Hence, one may expect significant spread of the conduction electrons in the **k** space along ⟨100⟩.

In the cubic phase of the Ba(Sr)TiO_3, the lowest lying t_{2g} conduction band is triply degenerate. The degeneracy is completely or partially removed by lowering of the crystal symmetry at the phase transition, spin-orbit coupling, symmetry-breaking point defects, uniaxial pressure, etc.[5] According to Mattheiss,[3] these effects can produce a complex multiple-band electronic structure at the bottom of the conduction band. In contrast to $SrTiO_3$, the Ti ion in $BaTiO_3$ is not located at the center of the O octahedra but is dynamically displaced along one of the ⟨111⟩ body diagonals. In the high-symmetry cubic phase, the position of the Ti ion is eightfold degenerate. Upon lowering the symmetry from the cubic to tetragonal, orthorhombic, and rhombohedral, the degeneracy of the Ti ion decreases to fourfold, twofold, and onefold, respectively.[6]

Undoped Ba(Sr)TiO_3 are band-gap insulators. The n-type conductivity in Ba(Sr)TiO_3 is realized either by reduction in oxygen-deficient atmosphere or by substituting for example, La^{3+} for $Ba^{2+}(Sr^{2+})$ or Nb^{5+} for Ti^{4+}. Due to the similar ionic radii of $Ba^{2+}(Sr^{2+})$ with La^{3+} and $Ti^{4+/3+}$ with $Nb^{5+/4+}$, Ba(Sr)TiO_3 forms complete solid solutions with $LaTiO_3$ and Ba(Sr)NbO_3.[7–10]

Transition from insulating to metallic (IM) behavior in $Sr_{1-x}La_xTiO_3$ and $SrTi_{1-y}Nb_yO_3$ single crystals occurs at rather small doping level e.g., $x<0.001$ (Ref. 11) and $y<0.0003$.[12] In contrast to Sr-based compounds, $Ba_{1-x}La_xTiO_3$ and $BaTi_{1-x}Nb_xO_3$ undergo IM transition at much higher doping levels, e.g., $x>0.15$.[7,10] The reason for such high doping levels is attributed either to disorder-induced Anderson-type localization[7] or phonon-induced localization[13] (i.e., small polaron model).

Unlike Nb and La dopants, both theory[14,15] and experiment[16] suggest that oxygen vacancy (V_O) is the strongest perturbation to the perovskite lattice which, for example, causes a collapse of the perovskite $BaTiO_{3-\delta}$ structure at the $[V_O]\geq1.5$ at %.[17] Upon doping with oxygen vacancies, $SrTiO_3$ undergoes an insulator-metal (IM) transition[18] at the critical electron concentration n_c of $10^{15}-10^{16}$ cm^{-3}. Optical,[19,20] magnetic,[21] and transport studies[22] indicate a strong electron-lattice interaction which causes enhancement of the electron effective mass m^* in n type $SrTiO_3$ (e.g., $m^*\approx4-16m_e$).

Although there have been reports on metallic conductivity of $BaTiO_{3-\delta}$ thin films,[23] neither n_c nor the charge transport properties of metallic $BaTiO_{3-\delta}$ single crystals have been systematically analyzed. Bearing in mind that the Ti ions in $BaTiO_3$ are dynamically off-centered, one may expect significant correlation between the electronic properties of n-type $BaTiO_3$ and temperature evolution of the crystallographic phases. In this work, the author used a scaled Mott criterion[24] ($n_c^{1/3}a_H^*\approx0.25$, where a_H^* is an effective Bohr radius of the isolated donor center) as a guide to find the IM transition in $BaTiO_{3-\delta}$. Despite its apparent simplicity, the criterion underscores the importance of the m^* and the static dielectric constant ε. Adopting literature data on $BaTiO_3$ (Ref. 25) (i.e., $m^*\approx6-12m_e$ and low temperature $\varepsilon\approx100$), one finds $a_H^*=4.4-7.6$ Å and $n_c=0.4-1.8\times10^{20}$ cm^{-3}. The

latter value agrees reasonably well with $n_c = 1.6 \times 10^{20}$ cm^{-3} experimentally found in this work.

The most puzzling result is that upon cooling below ca. 70 K, the dominant type of charge carriers in metallic $BaTiO_{3-\delta}$ changes from electrons to holes. This is in contrast to the $SrTiO_{3-\delta}$ which remains n type down to the lowest temperatures studied. It is proposed that both the sign reversal of the Hall and Seebeck coefficients as well as anomalous magnetism of metallic $BaTiO_{3-\delta}$ are the manifestations of the carrier contribution from the multiple electronic bands separated by the narrow gap.

II. EXPERIMENT

Nominally undoped $BaTiO_3$ single crystals of $10 \times 10 \times 1$ mm^3 cut along the (100) planes were purchased from K&R Creation Co., Ltd. The concentration of the typical paramagnetic impurities (e.g., Fe, Cr, Co, Mn, Ni, Pt, and Rh) of 10–15 ppm in the as-received samples was estimated from the low-temperature Curie-Weiss tail of the magnetic-susceptibility data adopting the average effective magnetic moment of impurities at 4.5 μ_B. The crystals were reduced in a tube furnace at 900–1250 °C in a flowing mixture of 5% H_2/95% N_2 or pure (99.999%) H_2 for 20–40 h. This treatment produced electron concentration ranging from 9.8×10^{17} to 3.5×10^{20} cm^{-3}. Reduction at higher temperatures resulted in a collapse of the perovskite structure and formation of hexagonal $BaTiO_{3-\delta}$ with the $P6_3/mmc$ space group.[26]

After reduction, the samples were cut into rectangles of ca. $10 \times 2 \times 1$ mm^3. Thermally evaporated Al electrodes were used to provide Ohmic contacts for four-probe resistivity ρ, Hall R_H, and Seebeck S, coefficients measurements. Hall effect was measured in the four-probe configuration by rotating the crystal by 180 deg in the magnetic field of 3 tesla. Magnetic susceptibility was measured on the crystals of ca. 180–200 mg with **H** parallel to the (100) crystal direction.

No attempts to prepare single domain crystals by polling in electric field have been made due to their high conductivity. However, for a weakly-reduced $BaTiO_{3-\delta}$, it was possible to identify single domain crystals in the T (tetragonal) phase, 270 K $< T <$ 403 K, after examination under polarized light. For intermediately doped $BaTiO_{3-\delta}$, the single domain crystals were determined *post factum* from the comparison of their $d(\ln \rho)/dT$ in the tetragonal phase with the resistivity data reported by Berglund and Baer[27] on single domain $BaTiO_{3-\delta}$. The resistivity in the tetragonal phase decreases (increases) with temperature when the electric current flows parallel (perpendicular) to the c axis. The domain pattern of the samples in the O (orthorhombic), 195 K $< T <$ 285 K, and R (rhombohedral), $T <$ 195 K, phases could not be identified unambiguously. The domain pattern for highly reduced samples 7 and 8 could not be unambiguously determined in the whole temperature range.

At the early stages of the experiment, it was found that the electric wires attached either by wire bonder or silver epoxy often detach from the sample due to a sudden contraction and/or expansion of the $BaTiO_3$ lattice when it passes through the phase-transition temperature. For resistivity measurements, this problem has been solved by using spring-loaded pin contacts[28] that ensured a stable electric contact with the crystals in the whole 2–400 K temperature range. However, for the Hall-effect measurements with QD PPMS rotator, the author had to use the wire bonder and often had to repeat the measurements due to the loss of electrical contact with the sample. At the same time, the author has tried to minimize the number of thermal cycling of the samples due to the cracking that occurs at the temperature of the phase transitions. For this reason, the Hall data for sample 5 in Fig. 2 have been reported only in the 200–400 K range. Nevertheless, the main conclusions of the paper are not significantly affected by this drawback.

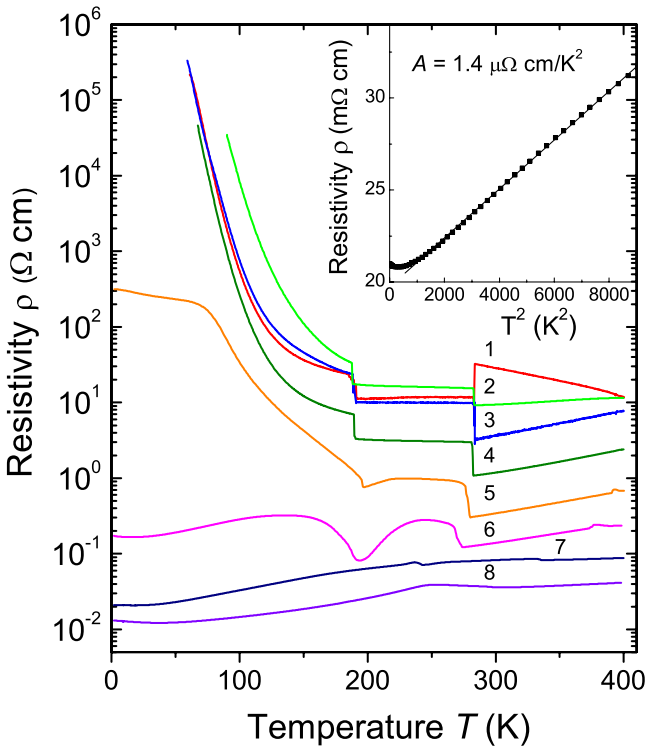

FIG. 1. (Color online) Dc resistivity of a series of the $BaTiO_{3-\delta}$ single crystals. Curves are labeled according to the data in Table I. Sample 1 was measured with $\mathbf{j} \| c$ and samples 3–6 were measured with $\mathbf{j} \| ab$ in the T (tetragonal) phase, 270 K $< T <$ 403 K. Sample 2 is a polydomain sample. The ferroelectric domain pattern of samples 7 and 8 could not be determined. The inset shows the low-temperature part of the ρ vs T^2 of sample 7.

III. RESULTS AND DISCUSSION

Figure 1 shows the $\rho(T)$ dependence of the $BaTiO_{3-\delta}$ crystals with various values of n specified in Table I. The $BaTiO_{3-\delta}$ samples undergo insulator-metal transition with increase in n. Samples with $n \leq 1 \times 10^{19}$ cm^{-3} have an insulating ground state with divergent resistivity as T approaches 0 K (curves 1–4 in Fig. 1). The $\rho(T)$ dependence of these samples in the rhombohedral (R) $T <$ 195 K phase has an activation energy $\varepsilon_{th} = 97-134$ meV estimated from the $\rho \propto \exp(\varepsilon_{th}/k_B T)$ relation. Crystals with intermediate doping

TABLE I. Physical parameters of the selected $BaTiO_{3-\delta}$ samples; n is the electron concentration at 400 K from the Hall-effect measurements, A is the T^2 coefficient of the resistivity of metallic $BaTiO_{3-\delta}$, μ_H is the Hall mobility at 400 K, and m^* is the density of states electron effective mass determined from the thermoelectric data at 400 K.

Sample	Preparation	n [10^{19} cm^{-3}]	A [$\mu\Omega$ cm/K^2]	μ_H [cm^2/Vs]	m^*/m_e
1–3	900 C, 40 h, 10 ccm H_2/N_2	0.098		0.52	12.5
4	900 C, 40 h, 40 ccm H_2/N_2	0.45		0.59	12.7
5	1000 C, 10 h, 40 ccm H_2/N_2	1.90		0.49	11.5
6	1050 C, 10 h, 40 ccm H_2	6.10	13.78	0.46	10.5
7	1100 C, 20 h, 90 ccm H_2	16.4	1.35	0.44	9.80
8	1250 C, 20 h, 90 ccm H_2	34.6	0.315	0.47	6.57

level, 1×10^{19} cm$^{-3}\leq n\leq 6\times10^{19}$ cm^{-3} (curves 5 and 6 in Fig. 1), develop a low-temperature $\rho(T)$ plateau below 100 K. Samples with $n\geq 1.6\times10^{20}$ cm^{-3} show metallic behavior (curves 7 and 8 in Fig. 1). The $\rho(T)$ of metallic samples can be fitted with the $\rho=\rho_0+AT^2$ relation with T extending up to 170 K (inset in Fig. 1). The T^2 dependence suggests that the electron-electron correlations play important role in metallic $BaTiO_{3-\delta}$, however, the large enhancement of A may be a signature of additional strong electron-phonon interaction.[29] This latter interaction is screened at higher n which explains a strong $A(n)$ dependence (see Table I).

Figure 2 shows temperature dependence of the Hall coefficient R_H ($R_H=1/en$). The samples with $n<1\times10^{19}$ cm^{-3} show weak temperature dependence of R_H in the 200–400 K. Below 180 K, in the R phase, the R_H diverges with decreasing T indicating freeze out of the charge carriers. The activation energy of n for insulating samples determined from the Hall data is around 94 meV (inset in Fig. 2) which is in good agreement with the activation energy determined from the $\rho(T)$ data. The values of the Hall mobility μ_H at 400 K are given in Table I. With an increase in n by three orders of magnitude, the μ_H shows very small decrease from 0.59 to 0.44 cm^2/Vs.

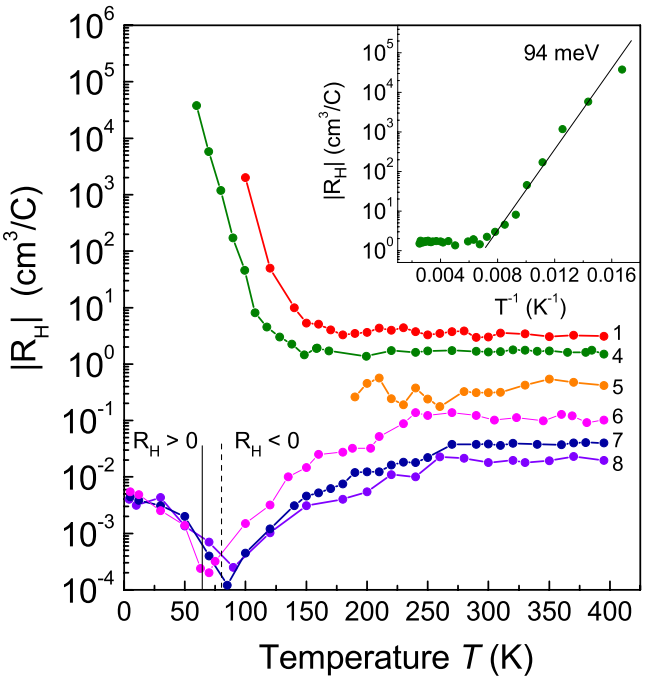

FIG. 2. (Color online) Temperature dependence of the Hall coefficient of the $BaTiO_{3-\delta}$ single crystals. Data are labeled according to the Table I. A crossover temperature from the high-T negative to low-T positive R_H is indicated by the vertical solid line for sample 6 and by dashed line for samples 7 and 8.

The most surprising result of the Hall data is an anomalous temperature dependence of the R_H of metallic samples. Above 290 K, the R_H of metallic $BaTiO_{3-\delta}$ is negative and nearly temperature independent in a similar way as that of the insulating samples. However, cooling below 290 K leads to a gradual decrease of the $|R_H|$ by two orders of magnitude. Below 75 K, the R_H takes positive values and remains positive down to 2 K (Fig. 2). This behavior is at variance with nearly temperature-independent R_H of metallic $SrTiO_{3-\delta}$.[22] Most importantly, it cannot be explained in terms of a single electron band model.

Temperature dependence of the Seebeck coefficient S is shown in Fig. 3. Crystallographic phase transitions in $BaTiO_{3-\delta}$ can be followed by steplike changes in the $S(T)$. Weakly doped samples (curve 1) show negative S in the 90–400 K range indicating that electrons are majority carriers. Below 90 K, the S is noisy due to the high resistance of the insulating samples. Strong enhancement of $S(T)$ below 300 K is explained by both freezing out of the charge carriers and significant phonon drag; another evidence of strong electron-phonon interactions in $BaTiO_3$. A very steep drop in $|S|$ below 100 K (curve 1) is peculiar feature of all insulating samples that can be a result of the variable range hopping ($S\propto T^{1/2}$) and a low-temperature component of the phonon drag ($S\propto T^3$).[30] This phenomenon warrants more detailed investigation which will be presented elsewhere. The effective mass of electrons m^* calculated from the Seebeck coefficient and the Hall-effect data at 400 K is presented in Table I. At this temperature, all the samples can be considered as nondegenerate semiconductors with Seebeck coefficient given by

$$S=\frac{k_B}{e}\left(\ln\frac{N_c}{n}+B\right), \tag{1}$$

where k_B is the Boltzmann constant, e is the electron charge, N_c is the effective density of states, and $B\approx 3$ is the electron-

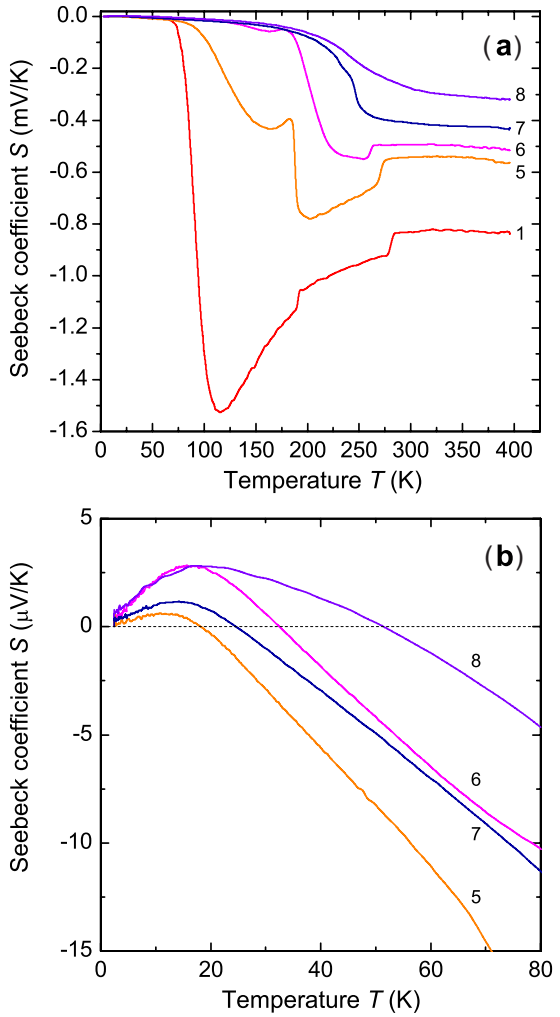

FIG. 3. (Color online) (a) Temperature dependence of the Seebeck coefficient. (b) Expanded view of the $S(T)$ dependence of metallic samples. Curves are labeled according to Table I.

scattering constant. Samples on the insulating side of the IM transition show m^* of the order of 12 m_e. Samples on metallic side of the IM transition show decrease in the m^* upon doping which could be an evidence of screening of the electron-phonon interaction and/or changes in the CB structure of metallic $BaTiO_{3-\delta}$.

Similar to the Hall data, the S of metallic $BaTiO_{3-\delta}$ undergoes major changes in the 100–300 K range. Remarkably, the Seebeck coefficient also changes sign from negative to positive [Fig. 3(b)] upon cooling below 60 K. It is noted that the temperature of the sign reversal is not constant but increases (except for sample 7) with concentration of the charge carriers. It is not immediately clear why sample 7 does not follow the trend. One of the reasons could be the different ferroelectric domain pattern of sample 7 that may affect the overall thermoelectric (and Hall effect) behavior. It was found that by repeating the thermoelectric power measurements, the temperature of the S sign reversal fluctuates within 5–10 degrees.

Another evidence of the complex electronic band structure of $BaTiO_{3-\delta}$ comes from the magnetic-susceptibility $\chi(T)$ data shown in Fig. 4. As expected, electron localization

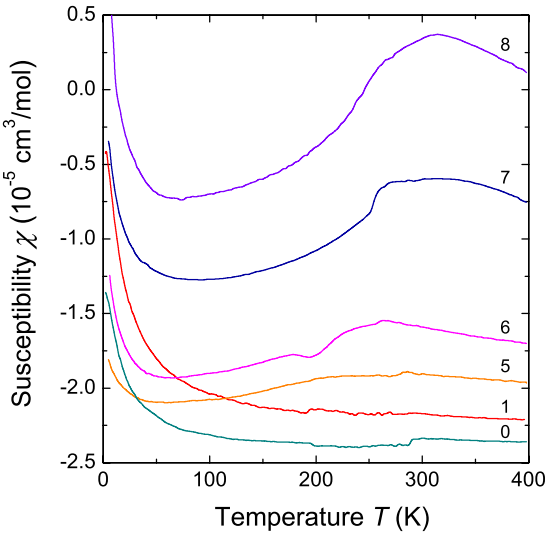

FIG. 4. (Color online) Temperature dependence of the molar magnetic susceptibility of a series of the $BaTiO_{3-\delta}$ single crystals. For comparison, curve 0 shows the $\chi(T)$ dependence of the undoped, as received $BaTiO_3$. All other curves are labeled according to Table I. The low-temperature paramagnetism of the 10–15 ppm of extrinsic impurities in sample 0 is manifested by the upturn of χ below 100 K. Small steplike changes in χ at the phase transitions are due the van Vleck paramagnetic contribution.

in the insulating samples (curve 1 in Fig. 4) is manifested by an increase in the Curie-Weiss paramagnetic contribution at low temperature. Transition from the localized to itinerant electron behavior is evidenced by a decrease in the χ values for the nearly metallic samples below 100 K (curves 5 and 6). In contrast to metallic $SrTiO_{3-\delta}$, which shows temperature-independent Pauli paramagnetism,[21] metallic $BaTiO_{3-\delta}$ (curves 7 and 8) show a broad maximum in $\chi(T)$. There is a certain analogy between the $\chi(T)$ behavior and the temperature dependencies of the R_H and S of metallic $BaTiO_{3-\delta}$. With an increase in n, the χ_{max} shifts to higher temperatures and the $\chi(T)$ anomaly becomes more pronounced.

The origin of the low-temperature p-type conduction in metallic $BaTiO_{3-\delta}$ cannot be attributed to the electron vacancy transport within the "impurity band." As explained in detail by Mott and Twose,[31] impurity band conduction in the n-type material will not have a p-type character because electron vacancy in the impurity band will always move in the opposite direction to the electron even in the magnetic field. Thus, the author suggests that the low-temperature p-type conduction in $BaTiO_{3-\delta}$ is an evidence of the two-band electronic structure of the conduction band. It is proposed that in the low-symmetry phase of $BaTiO_3$, the bottom of the CB is split into lower and upper bands separated by a small energy gap. The reported properties of metallic $BaTiO_{3-\delta}$ are controlled by the thermally-activated occupation of these two bands with electrons. At low temperatures, the carrier transport and magnetic susceptibility are dominated by the lower band which is almost completely filled with electrons. This would result in the positive sign of the Hall and Seebeck coefficients at low T. Owing to a relatively low sign crossover temperature, the energy gap separating

the lower and upper bands is of the order of 3–7 meV (i.e., 30–75 K). Therefore, at $T \geq 300$ K, the electronic and magnetic properties of metallic $BaTiO_{3-\delta}$ are dominated by the electrons thermally excited to the upper band.

In conclusion, the author reports on the IM transition in the $BaTiO_{3-\delta}$ and suggests a two-band conduction model to explain the low-temperature *p*-type conductivity and anomalous magnetic properties of metallic $BaTiO_{3-\delta}$. It is expected that at low T, the off-center displacement of the Ti ions as well as the low-symmetry structure of the $BaTiO_3$ lattice will remove the threefold degeneracy of the t_{2g} band and will result in a rather complex Fermi surface. Donor dopants, in particular oxygen vacancies, can significantly modify the CB structure of $BaTiO_3$. Recent theoretical studies on $Ba(Sr)TiO_3$ point out that the ground-state orbital configuration of the Ti ions residing next to the V_O is no longer of the t_{2g} but rather of the e_g type.[15] This eventually may result in the formation of the multiple Fermi surfaces centered, for example, at the X and the Γ points of the Brillouin zone. First-principles calculations of the low-symmetry phases of $BaTiO_{3-\delta}$ that explicitly take into account the off-center dynamic displacements of Ti ions would be extremely useful to clarify the author's hypothesis.

ACKNOWLEDGMENTS

The author thanks I. Solov'yev, M. Tachibana, R. Scipioni, M. Boero, S. Wimbush, and Y. Endoh for stimulating discussions and interest in this work. This study was supported by MEXT, Japan.

*kolodiazhnyi.taras@nims.go.jp

[1] E. A. Stern, Phys. Rev. Lett. **93**, 037601 (2004); B. Zalar, A. Lebar, J. Seliger, R. Blinc, V. V. Laguta, and M. Itoh, Phys. Rev. B **71**, 064107 (2005); B. Zalar, V. V. Laguta, and R. Blinc, Phys. Rev. Lett. **90**, 037601 (2003); T. Kolodiazhnyi and S. C. Wimbush, *ibid.* **96**, 246404 (2006); B. Ravel, E. A. Stern, R. I. Vedrinskii and V. Kraisman, Ferroelectrics **206**, 407 (1998).

[2] A. H. Kahn and A. J. Leyendecker, Phys. Rev. **135**, A1321 (1964).

[3] L. F. Mattheiss, Phys. Rev. B **6**, 4740 (1972).

[4] E. Heifets, E. Kotomin, and V. A. Trepakov, J. Phys.: Condens. Matter **18**, 4845 (2006).

[5] S. Lenjer, O. F. Schirmer, H. Hesse, and Th. W. Kool, Phys. Rev. B **66**, 165106 (2002).

[6] J. P. Itié, B. Couzinet, A. Polian, A. M. Flank, and P. Lagarde, Europhys. Lett. **74**, 706 (2006).

[7] V. Fritsch, J. Hemberger, M. Brando, A. Engelmayer, S. Horn, M. Klemm, G. Knebel, F. Lichtenberg, P. Mandal, F. Mayr, M. Nicklas, and A. Loidl, Phys. Rev. B **64**, 045113 (2001).

[8] P. Mandal, Phys. Rev. B **71**, 165106 (2005).

[9] R. Moos, S. Schöllhammer, and K. H. Härdtl, Appl. Phys. A: Mater. Sci. Process. **65**, 291 (1997).

[10] J. F. Marucco, M. Ocio, A. Forget, and D. Colson, J. Alloys Compd. **262-263**, 454 (1997).

[11] H. Suzuki, H. Bando, Y. Ootuka, I. H. Inoue, T. Yamamoto, K. Takahashi, and Y. Nishihara, J. Phys. Soc. Jpn. **65**, 1529 (1996).

[12] H. P. R. Frederikse, W. R. Thurber, and W. R. Hosler, Phys. Rev. **134**, A442 (1964).

[13] T. Holstein, Ann. Phys. (N.Y.) **8**, 343 (1959).

[14] J. P. Buban, H. Iddir and S. Öğüt, Phys. Rev. B, **69**, 180102(R) (2004).

[15] W. Luo, W. Duan, S. G. Louie, and M. L. Cohen, Phys. Rev. B **70**, 214109 (2004); H. Donnerberg and A. Birkholz, J. Phys.: Condens. Matter **12**, 8239 (2000); C. H. Park and D. J. Chadi, Phys. Rev. B **57**, R13961 (1998); D. Ricci, G. Bano, G. Pacchioni, and F. Illas, *ibid.* **68**, 224105 (2003); D. D. Cuong, B. Lee, K. M. Choi, H.-S. Ahn, S. Han, and J. Lee, Phys. Rev. Lett. **98**, 115503 (2007).

[16] K. H. Härdtl and R. Wernicke, Solid State Commun. **10**, 153 (1972).

[17] D. C. Sinclair, J. M. S. Skakle, F. D. Morrison, R. I. Smith, and T. P. Beales, J. Mater. Chem. **9**, 1327 (1999).

[18] D. Parker and J. Yahia, Phys. Rev. **169**, 605 (1968).

[19] F. Gervais, J. L. Servoin, A. Baratoff, J. G. Bednorz, and G. Binnig, Phys. Rev. B **47**, 8187 (1993).

[20] J. L. M. van Mechelen, D. Vandermarel, C. Grimaldi, A. Kuzmenko, N. Armitage, N. Reyren, H. Hagemann, and I. Mazin, Phys. Rev. Lett. **100**, 226403 (2008).

[21] H. P. R. Frederikse and G. A. Candela, Phys. Rev. **147**, 583 (1966).

[22] H. P. R. Frederikse, W. R. Hosler, and W. R. Thurber, Phys. Rev. **143**, 648 (1966).

[23] T. Zhao, Z.-H. Chen, F. Chen, H.-B. Lu, G.-Z. Yang, and H.-S. Cheng, Appl. Phys. Lett. **77**, 4338 (2000).

[24] P. P. Edwards and M. J. Sienko, Phys. Rev. B **17**, 2575 (1978).

[25] M. Yamamoto, H. Ohta, and K. Koumoto, Appl. Phys. Lett. **90**, 072101 (2007).

[26] T. Kolodiazhnyi, A. A. Belik, S. C. Wimbush, and H. Haneda, Phys. Rev. B **77**, 075103 (2008).

[27] C. N. Berglund and W. S. Baer, Phys. Rev. **157**, 358 (1967).

[28] http://ppms.atspace.com/

[29] G.-M. Zhao, V. Smolyaninova, W. Prellier, and H. Keller, Phys. Rev. Lett. **84**, 6086 (2000).

[30] P. M. Chaikin, in *Organic Superconductivity*, edited by V. Z. Kresin and W. A. Little (Plenum, New York, 1990), p. 101.

[31] N. F. Mott and W. D. Twose, Adv. Phys. **10**, 107 (1961).